1 January 2002

ELSEVIER

Optics Communications 201 (2002) 21–28

OPTICS COMMUNICATIONS

www.elsevier.com/locate/optcom

Revolving interference patterns for the rotation of optically trapped particles

M.P. MacDonald *, K. Volke-Sepulveda, L. Paterson, J. Arlt, W. Sibbett, K. Dholakia

The School of Physics and Astronomy, St. Andrews University, North Haugh, St. Andrews, Fife KY16 9SS, Scotland, UK

Received 27 June 2001; received in revised form 19 September 2001; accepted 16 October 2001

Abstract

Optically trapped objects are rotated controllably in the interference pattern between a Laguerre–Gaussian (LG) beam and a Gaussian beam. In this work the interference pattern is analysed and its properties as it propagates are modelled, showing the important role played by the Guoy-phase of the two interfering beams. An analysis of producing controlled rotation of the interference pattern using a glass plate is presented demonstrating the ease with which the rotation can be controlled.

PACS: 42.40.Eq; 42.60.Jf; 42.62.Be; 42.79.Yd

Keywords: Optical trapping; Optical manipulation; Laguerre–Gaussian beams; Interference patterns; Micro-particle rotation

1. Introduction

Optical manipulation and confinement of microscopic particles is a powerful technique that has found many applications in its short history, particularly in biology. In this technique the optical "gradient" or dipole force attracts microscopic particles to the region of highest light intensity such that a tightly focused light beam can trap a microscopic particle in three dimensions. These "optical tweezers" pioneered by Ashkin and co-workers [1–3] have seen many advances in the decade since their first demonstration, each of which has increased the scope of optical micro-manipulation.

In addition to the ability to translate a particle in three dimensions, the freedom to rotate optically trapped particles has attracted a lot of attention recently. Optically induced rotation offers a non-contact mechanism for driving optical micro-machines and micro-components such as cogs [4,5]. From a biological viewpoint rotation of trapped particles offers the ability to easily orient biological specimens such that active sites on enzymes attached to beads could be aligned to latch onto one another. Several schemes have been proposed and implemented to induce particle rotation at the microscopic level. For example, spe-

* Corresponding author. Tel.: +44-1334-463184; fax: +44-1334-463104.

E-mail address: mpm4@st-and.ac.uk (M.P. MacDonald).

0030-4018/02/$ - see front matter
PII: S0030-4018(01)01652-2

cially fabricated microscopic components can rotate due to the manner in which the light is scattered from the component [6–8] or a revolving laser pattern can be used to rotate optically trapped particles [9]. Schemes have also been realised where either the spin or orbital angular momentum of light can be transferred to a trapped particle. The transfer of orbital angular momentum can be achieved by partial absorption of the trapping light, though this leads to undesirable heating of the tweezed particle [10–13]. Spin angular momentum can be transferred to trapped birefringent particles without any absorption and can lead to high rotation rates in a manner similar to Beth's original experiment [14–17]. This technique can also be used to align and controllably rotate birefringent particles [18].

In recent work, we have introduced an alternative scheme to rotate tweezed particles that does not rely on specific particle properties [19]. This technique uses the ability to trap microscopic particles in an interference pattern [20,21]. Specifically we have trapped objects (in 2D) in the interference pattern between a suitable Laguerre–Gaussian (LG) beam and a Gaussian beam [22]. By changing the path length of one of the beams we are able to cause the interference pattern (and thus the trapped particles) to rotate in a controlled fashion about the axis of the spiral pattern. This rotation is due to the helical nature of the wavefronts of an LG light beam [23].

In this paper we describe in detail how the pattern evolves as it propagates and how the Guoy-phase shift affects the shape of the pattern as it is focussed to achieve optical trapping. Possible aberrations in the pattern arising from various forms of misalignment are discussed, showing that the pattern is fairly resilient to such misalignment. The manner in which a glass plate can be used to controllably produce rotations in the pattern is modelled and compared to actual results.

2. Interference pattern between a Laguerre–Gaussian and Gaussian beam

An LG beam has two mode indices to fully describe the mode: l and p. A given mode will have l complete cycles of phase (2π) upon going around the mode circumference so that l is known as the azimuthal index. The index p gives the number $(p+1)$ of radial nodes. LG light beams are well known to possess orbital angular momentum in the light beam due to an $e^{il\phi}$ phase term in the mode description where Φ is the azimuthal phase [23]. This angular momentum of magnitude of $l\hbar$ is distinct from the spin angular momentum due to the polarisation state of the light. The full mode description is given by Eq. (1),

$$E(\mathrm{LG}_p^l) \propto \exp\left[\frac{-\mathrm{i}kr^2}{2(z_\mathrm{R}^2+z^2)}\right]\exp\left[\frac{-r^2}{\omega^2}\right] \times \exp\left[-\mathrm{i}(2p+|l|+1)\arctan\left(\frac{z}{z_\mathrm{R}}\right)\right] \times \exp[-\mathrm{i}l\Phi]\times\left(\frac{r\sqrt{2}}{\omega}\right)^{|l|} L_p^{|l|}\left(\frac{2r^2}{\omega^2}\right), \quad (1)$$

where z is the distance from the beam waist, z_R is the Rayleigh range, k is the wave number, ω is the Gaussian beam waist, r is the radius and $L_p^{|l|}$ is the generalised Laguerre polynomial [13]. Several methods exist for generating LG beams including the use of a spiral phase plate [24] or the direct formation of the beam inside a laser resonator [25,26]. However, the most practical methods are the use of a mode converter to transform a higher-order Hermite–Gaussian beam into an LG beam [27] and the use of holographic elements [28–32]. The mode converter results in a pure LG beam but the holographic method is more versatile in that one only needs to illuminate the hologram with a TEM_{00} mode and conversion efficiencies in excess of 75% are possible. However, the output mode from a hologram is a superposition of various modes of different p but the same azimuthal index l [32].

Using a hologram to produce the LG beam results in the LG beam having a different beam waist from the incident Gaussian beam [29]. The difference between the beam waists of the incident beam on the hologram ω_0^{in} and the LG beam produced ω_0^{out} (input and output beams) is given by Eq. (2):

$$\frac{\omega_0^{\mathrm{out}}}{\omega_0^{\mathrm{in}}} = \frac{1}{\sqrt{|l|+1}}. \quad (2)$$

On examination of Eq. (1) it is seen that the phase fronts of the beam describe a helix with l intertwined surfaces. Hence for $p = 0$ the phase fronts of an LG $l = 2$ beam will be a double start helix and an $l = 3$ beam will be a triple start helix. A helix with index l will repeat every $l\lambda$. In this study we limit our discussion to single-ringed ($p = 0$), LG beams.

The Guoy-phase shift $\Phi^{\mathrm{LG}}_{\mathrm{Guoy}}$ (Eq. (3)) gives the perturbation near a focus of the propagating helical phase fronts from that of a spherical wave:

$$\Phi^{\mathrm{LG}}_{\mathrm{Guoy}} = (2p + |l| + 1)\arctan\left(\frac{z}{z_{\mathrm{R}}}\right). \tag{3}$$

The matching mode description for a fundamental Gaussian beam however is given by Eq. (1) when $l = 0$ and $p = 0$, hence the Guoy-phase shift $\Phi^{\mathrm{G}}_{\mathrm{Guoy}}$ is now just $\arctan(z/z_{\mathrm{R}})$. So we see that both the curvature of the wavefronts of the LG and Gaussian beams and their Guoy-phase shifts will be different.

By interfering an LG beam with a Gaussian beam the azimuthal phase variation of the LG beam is transformed into an azimuthal intensity variation with l nodes. A simulation of the pattern produced by interfering a Gaussian beam and an LG beam of azimuthal index $l = 3$ as the pattern travels through a focus is shown in Fig. 1. This is shown for $\omega_0^{\mathrm{G}} = 2\omega_0^{\mathrm{LG}}$ which is the ratio of the beam waists for an $l = 3$ LG beam as determined from Eq. (2). It can be seen that the pattern has a spiral shape, which is a result of the mismatch between the curvatures of the LG and Gaussian wavefronts. The interference pattern will always have a spiral shape unless the wavefronts of the two beams have the same curvature, such as at a focus, in which case the pattern will look like l intense spots of light. An example of this is shown in Fig. 1 where the pattern reduces to a set of three spots at the focus. Fig. 1 also shows the spiral pattern rotating slightly as it propagates through the focus. This is due to the differences between the Guoy-phase shifts Φ_{Guoy} of the LG and Gaussian beams [33]. A further effect is the reversal of the sense of the spiral as it passes through the focus. This is due to the reversal of the curvature of the wavefronts and does not affect the sense of rotation of the spiral due to the Guoy-phase shift mismatch.

The pattern is fairly resilient to beam misalignment as is shown in simulations in Fig. 2 where the beam has been displaced in three different ways. In Fig. 2(a) the Gaussian beam has half the beam waist ω_0 of the LG beam which makes it difficult to resolve the pattern at the focus, Fig. 2(b) shows the effect of the Gaussian beam coming to a focus earlier than the LG beam by $5z_{\mathrm{R}}$ (Rayleigh range of the LG beam) and Fig. 2(c) shows the effect of a transverse misalignment of the beams by a whole LG beam radius ω_0.

Though the intensity cross-section of the interference pattern changes slightly in space as the beam propagates, in the absence of a frequency separation between the two beams, the pattern does not change in time unless the relative phase of the beams is changed in time. If we do change the relative axial phase of the two beams in time the interference pattern will rotate around the beam axis. As an analogy, this is akin to considering what occurs along a length of rope that consists of

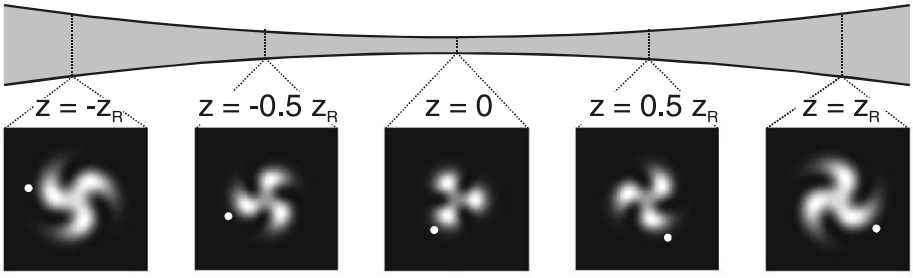

Fig. 1. Propagation of the spiral interference pattern through a focus. The white dot indicates the rotation of the pattern due to the different Guoy-phase shifts of equal intensity LG ($l = 3$) and Gaussian beams when the beam waists are related by $\omega_0^{\mathrm{G}} = 2\omega_0^{\mathrm{LG}}$.

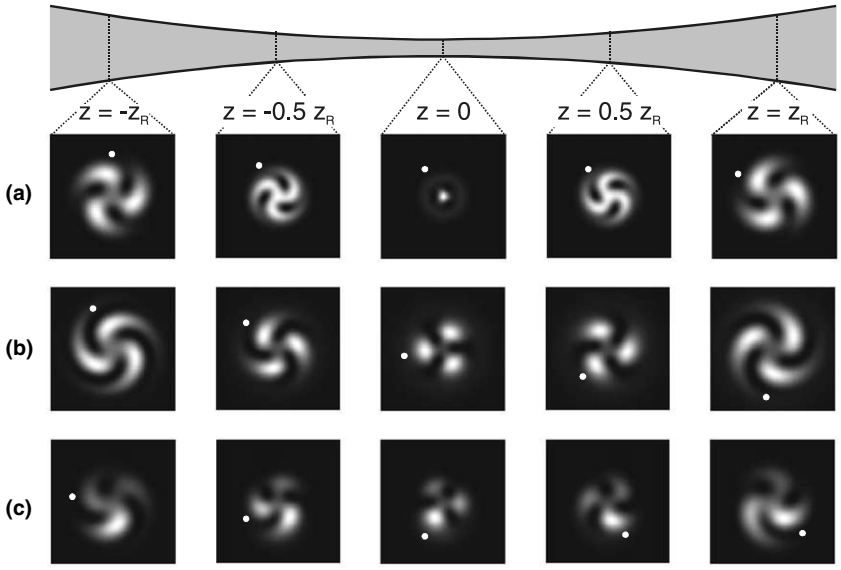

Fig. 2. Pattern aberations when a Gaussian beam is misaligned with respect to an LG $l = 3$ beam: (a) $\omega_0^{\mathrm{G}} = \frac{\omega_0^{\mathrm{LG}}}{2}$; (b) focus longitudinally displaced by $5z_{\mathrm{R}}^{\mathrm{LG}}$ and (c) transversely displaced by ω_0^{LG}.

l intertwined cords (see Fig. 3(a)). If you look at the cross-section of the rope as you travel along it the individual cords appear to rotate around the axis of the rope. Moving along the rope like this is analogous to altering the optical path length of one of the interfering beams, hence the spiral pattern as observed at a fixed plane in space can be rotated by changing the path length of one of the two interfering beams (see Fig. 3(b)). The helix of the phase in the LG beam repeats every $l\lambda$, thus a path length change in one beam of $l\lambda$ will cause the pattern to rotate through 360°. The fact that the pattern propagates and rotates evenly at every cross-section of the interfering beams suggests that it is suitable for achieving z-trapping in optical tweezers. This is in contrast to a pattern produced by simply imaging a shaped aperture, where there is little or no propagation of the pattern. It is worth noting that using patterns produced from LG beams of differing azimuthal index offers the

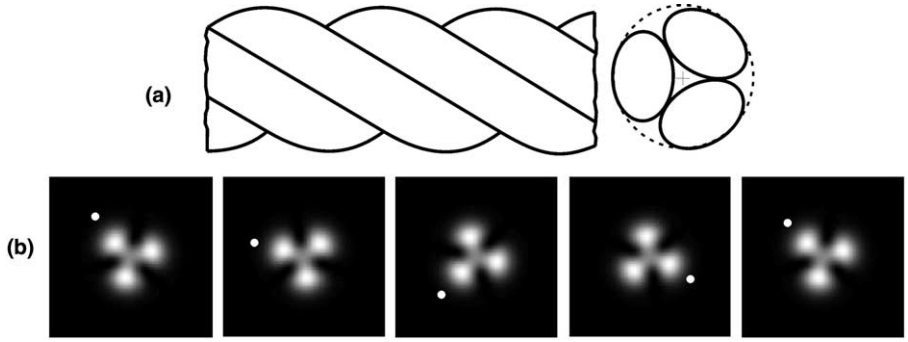

Fig. 3. (a) *Analogy*: rope consisting of three intertwined cords analogous to the phase of an LG beam with azimuthal index $l = 3$. (b) *Simulation*: the rotation of the interference pattern at a focus as the path length of one of the beams is changed. The white dot indicates the anti-clockwise rotation.

prospect of trapping and rotating different shaped objects and groups of objects [34].

3. Producing pattern rotation

The interference pattern between an LG beam and a Gaussian beam can be made to rotate around the axis of the beam by displacing the two beams either through a change in the relative longitudinal (axial) phase of the two beams or by creating a frequency difference between the two beams.

The frequency of one of the beams can be shifted by as little as a few H_2, through the use of two acousto-optic modulators (one to step the frequency up and the other to shift it back down). This causes the pattern to rotate continuously at a rate directly related to the beat frequency between the two beams. Through control of the frequency shift between the two beams the sense and speed of rotation could be accurately controlled, making this technique the most suited to the situation where continuous or high repetition rate rotation is desired.

Control of the relative longitudinal phase between the LG and Gaussian beams can be achieved by manipulating the path length in one arm of the interferometer using for example: the piezo-electric activation of a mirror in the interferometer, the rotation of a radial phase plate in one arm of the interferometer, with the aid of an LCD phase actuator or simply through the tilting of a glass plate. This can give very accurate alignment of the pattern and a high degree of control over any particle trapped within it.

The technique used in this work was the simplest of the above, namely the tilting of a glass plate. What follows is an analysis of the use of a glass plate for giving a limited number of rotations in the pattern.

The necessary parameters for calculating the effect of tilting the glass plate are shown in Fig. 4. The change in path length Δ produced by a tilt angle θ ($\theta = \phi_i$) in the glass plate is given by Eq. (4):

$$\Delta = t\left\{n\left(\frac{1}{\cos\varphi_r} - 1\right) + 1 - \frac{\cos(\theta - \varphi_r)}{\cos\varphi_r}\right\}. \quad (4)$$

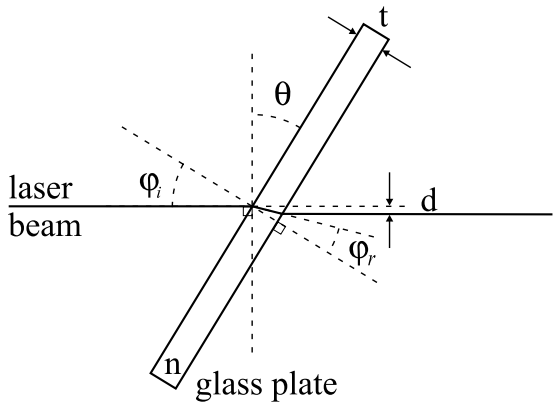

Fig. 4. Schematic of a glass plate showing the relevant parameters: ϕ_i, angle of incidence; ϕ_r, angle of refraction; d, beam deflection; t, plate thickness and n, refractive index of glass plate.

Applying Snell's Law, it is possible to determine ϕ_r and hence the number of rotations N produced in the spiral interference pattern from Eq. (5),

$$N = \frac{\Delta}{l\lambda}, \quad (5)$$

where l again is the azimuthal index of the LG beam and λ is the wavelength. For the purposes of accurate alignment of the beam it is more useful to express rotation as an angle a in radians: $\alpha = 2\pi N$. There is a resultant displacement d in the beam which can be found from Eq. (6),

$$d = t\frac{\sin(\theta - \varphi_r)}{\cos\varphi_r}, \quad (6)$$

though there is no angular deflection so long as the sides of the plate are parallel. It is clear that both the number of rotations the glass plate can induce in the spiral and the resultant deflection of the beam are directly proportional to the plate thickness t. This means that the ratio N/d is always the same for a given tilt angle. The rotation of the pattern and the lateral displacement of the beam as the glass plate is tilted are shown in Fig. 5. The rotations achieved in an $l = 2$ interference pattern from tilting a glass microscope slide and cover glass are shown in Fig. 6 where we see very good agreement with theory. One full rotation of the $l = 3$ spiral is shown in Fig. 3 as a result of tilting the glass plate through 8° from the normal. Since

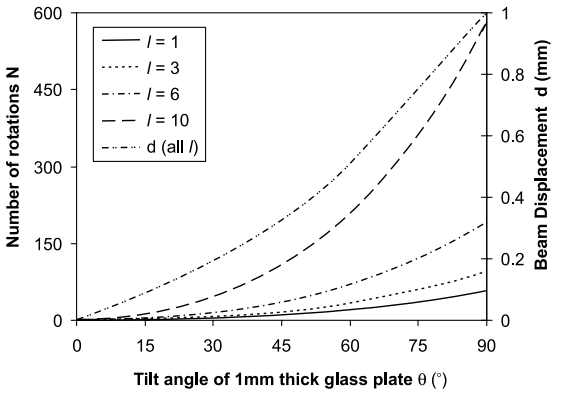

Fig. 5. Number of rotations N of the spiral patterns and displacement d of the beam as the glass plate is tilted.

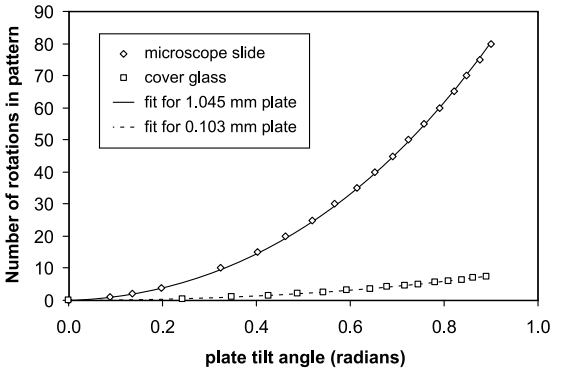

Fig. 6. The diamonds and squares show the number of rotations measured in an LG $l = 2$ interference pattern as a glass microscope slide and a glass cover slip are tilted from normal. The line curves show Eq. (5) for a glass plate of thickness $t = 1.04$ mm and cover glass $t = 0.103$ mm.

the displacement d is not proportional to the number of rotations N, the displacement that results from a given number of rotations will be different depending on what tilt angle the glass plate has as a starting angle. In practice the smallest displacement possible should be sought and this is found when tilting the glass plate from normal ($\theta = 0°$).

It is clear that the number of rotations achievable is greater for a thicker plate but that the possible displacement is also larger. A further consideration is that a thick plate requires a smaller angle of rotation to create the same number of rotations as a thin plate but for a given

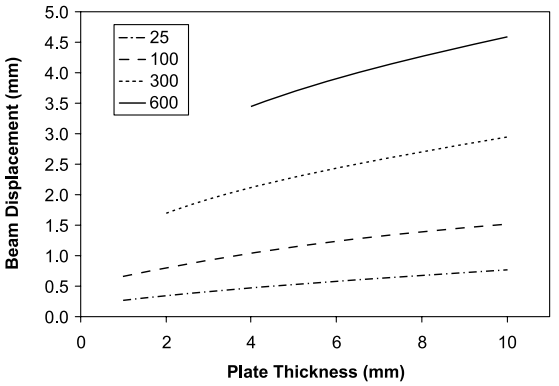

Fig. 7. The displacement d for various values of N (for values given in legend) as the plate thickness t is varied for an $l = 3$ interference pattern.

maximum desired number of rotations it is always best to take the thinnest plate available to avoid undue displacement of the beam. This is illustrated in Fig. 7 which shows continually increasing values of displacement d with plate thickness t for the $l = 3$ interference pattern when the plate is tilted from the normal. It can also be seen that the displacement becomes very large if high numbers of rotations are made.

In summary the use of a glass plate to produce the rotation in the interference pattern (and hence the trapped particles) is most suitable when the number of rotations required is limited. If a maximum required number of rotations is known, then the thinnest plate that can achieve this number of rotations should be used. If continuous rotation of the pattern is necessary then a method such as the AOM technique, for giving rotation rates related to the beat frequency between two frequency shifted beams, should be used.

4. Experiment

The experimental setup used was equivalent to that seen in [19] and is shown in Fig. 8. A holographically produced LG beam was interfered with the zeroth-order beam in order to generate the interference pattern which was then directed into a microscope using a 40× objective such that objects could be trapped and rotated.

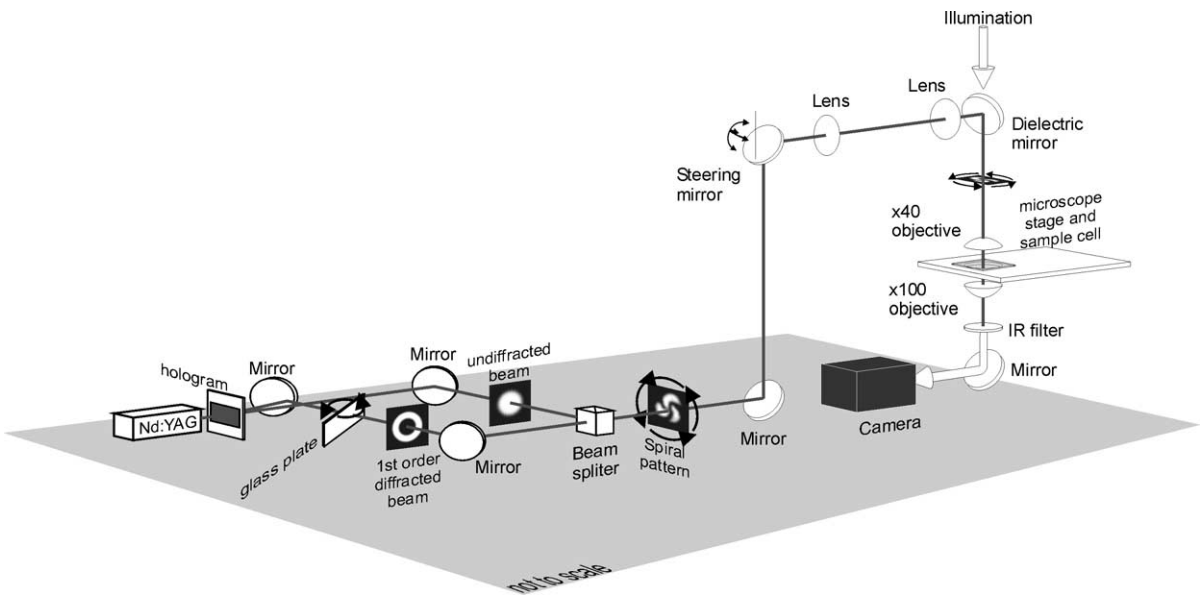

Fig. 8. Experimental setup for rotating microscopic objects in a spiral interference pattern.

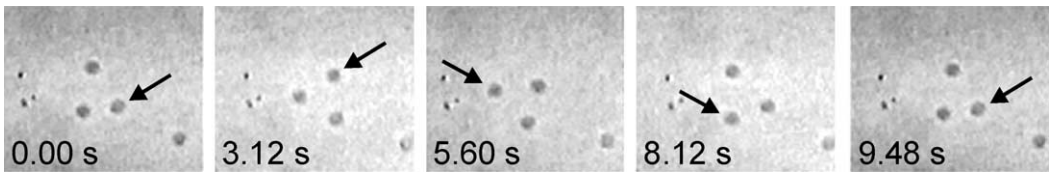

Fig. 9. Three 1 μm diameter silica spheres being rotated in the interference pattern produced with an LG $l = 3$ beam. One of the beads is tracked with an arrow.

The rotation of trapped particles in an interference pattern between an LG ($l = 3$) mode and a Gaussian beam can be seen in Fig. 9, where we see three trapped 1 μm silica spheres rotate in this pattern. One of the spheres is tracked in the images and the series of pictures charts the progress of this structure of spheres as the pattern is rotated. We note that DNA could be attached between these spheres in order to position and stretch the molecule [35] or the spheres could be attached to proteins such as the motor protein kinesin in order to measure their working strokes [36]. Spheres have also been rotated in closely packed groups of two or three [19]. The two sphere arrangement required the use of an $l = 2$ LG interference pattern which was also used to rotate microscopic glass rods and Chinese hamster chromosomes [19].

5. Conclusion

In conclusion, we have analysed the propagation of the interference pattern produced between an LG beam and a Gaussian beam as they pass through a focus. We have shown how this pattern could be controllably rotated with particular attention to tilting a glass plate showing that this was especially suited to the situation where a limited number of rotations in trapped sample are required. This gives better understanding of how these beam can be used to controllably rotate optically trapped microscopic particles using an interference pattern. As a further demonstration of the power of this technique we have shown the controlled rotation of an open structure of three trapped silica

spheres. The method is a fully controllable, non-invasive technique which should find widespread applications in generating optical and biological micromachines.

Acknowledgements

The authors would like to thank Fritz Akerboom for preparing the glass rods and the Engineering and Physical Science Research Council (EPSRC) for their support. K.V.-S acknowledges the support of CONACYT, Mexico and Dr. Sabino Chávez-Cerda.

References

[1] A. Ashkin, J.M. Dziedzic, Appl. Phys. Lett. 19 (1971) 283.
[2] A. Ashkin, J.M. Dziedzic, J.E. Bjorkholm, S. Chu, Opt. Lett. 11 (1986) 288.
[3] A. Ashkin, J.M. Dziedzic, T. Yamane, Nature 300 (1987) 6150.
[4] R.C. Gauthier, R.N. Tait, H. Mende, C. Pawlowicz, Appl. Opt. 40 (2001) 930.
[5] M.E.J. Friese, H. Rubenstein-Dunlop, J. Gold, P. Hagberg, D. Hanstorp, Appl. Phys. Lett. 78 (2001) 547.
[6] P. Galajda, P. Ormos, Appl. Phys. Lett. 78 (2000) 249.
[7] E. Higurashi et al., Appl. Phys. Lett. 64 (1994) 2209.
[8] E. Higurashi et al., J. Appl. Phys. 82 (1997) 2773.
[9] S. Sato et al., Electron. Lett. 27 (1991) 1831.
[10] H. He, M.E.J. Friese, N.R. Heckenberg, H. Rubinsztein-Dunlop, Phys. Rev. Lett. 75 (1995) 826.
[11] M.E.J. Friese, J. Enger, H. Rubinsztein-Dunlop, N.R. Heckenberg, Phys. Rev. A 54 (1996) 1593.
[12] N.B. Simpson, K. Dholakia, L. Allen, M.J. Padgett, Opt. Lett. 22 (1997) 52.
[13] N.B. Simpson, L. Allen, M.J. Padgett, J. Mod. Opt. 43 (1996) 2485.
[14] R.A. Beth, Phys. Rev. 50 (1936) 115.
[15] M.E.J. Friese, T.A. Nieminen, N.R. Heckenberg, H. Rubinsztein-Dunlop, Nature 394 (1998) 348.
[16] D.N. Moothoo, J. Arlt, R.S. Conroy, F. Akerboom, A. Voit, K. Dholakia, Am. J. Phys. 69 (2000) 271.
[17] E. Higurashi, R. Sawada, T. Ito, Appl. Phys. Lett. 73 (1998) 3034.
[18] E. Higurashi, R. Sawada, T. Ito, Phys. Rev. E 59 (1999) 3676.
[19] L. Paterson, M.P. MacDonald, J. Arlt, W. Sibbett, P.E. Bryant, K. Dholakia, Science 292 (2001) 912.
[20] A.E. Chiou, W. Wang, G.J. Sonek, J. Hong, M.W. Berns, Opt. Commun. 133 (1997) 7.
[21] M.P. MacDonald, L. Paterson, J. Arlt, W. Sibbett, P. Bryant, K. Dholakia, Opt. Lett. 26 (2001) 863.
[22] M. Padgett, J. Arlt, N. Simpson, L. Allen, Am. J. Phys. 64 (1996) 77.
[23] L. Allen, M.W. Beijersbergen, R.J.C. Spreeuw, J.P. Woerdman, Phys. Rev. A 45 (1992) 8185.
[24] M.W. Beijersbergen, R.P.C. Coerwinkel, M. Kristensen, J.P. Woerdman, Opt. Commun. 112 (1994) 321.
[25] R. Oron, N. Davidson, A.A. Friesem, F. Hasman, Opt. Commun. 182 (2000) 205.
[26] R. Oron, S. Blit, N. Davidson, A.A. Friesem, Z. Bomzon, E. Hasman, Appl. Phys. Lett. 77 (2000) 3322.
[27] M.W. Beijersbergen, L. Allen, H.E.L.O. Vanderveen, J.P. Woerdman, Opt. Commun. 96 (1993) 123.
[28] K.T. Gahagan, G.A. Swartzlander, Opt. Lett. 21 (1996) 827.
[29] M.A. Clifford, J. Arlt, J. Courtial, K. Dholakia, Opt. Commun. 156 (1998) 300.
[30] E.R. Dufresne, G.C. Spalding, M.T. Dearing, S.A. Sheets, D.G. Grier, Rev. Sci. Inst. 72 (2001) 1810.
[31] J. Gluckstadt, Opt. Commun. 175 (2000) 75.
[32] N.R. Heckenberg, R. McDuff, C.P. Smith, H. Rubinsztein-Dunlop, M.J. Wegener, Opt. Quant. Electron. 24 (1992) S951.
[33] R. Piestun, Y.Y. Schechner, J. Shamir, J. Opt. Soc. Am. A 17 (2000) 294.
[34] Y.Y. Schechner, R. Piestun, J. Shamir, Phys. Rev. E 54 (1996) R50.
[35] C. Bustamante, J.F. Marko, E. Siggia, S. Smith, Science 265 (1994) 1599.
[36] K. Svoboda, C.F. Schmidt, B.J. Schnapp, S.M. Block, Nature 365 (1993) 721.